Cockcroft-11-27

THIN FOIL-BASED SECONDARY EMISSION MONITOR FOR LOW INTENSITY, LOW ENERGY BEAM PROFILE MEASUREMENTS

J. Harasimowicz, C.P. Welsch, Cockcroft Institute and University of Liverpool, UK
J.L. Fernandez-Hernando, Cockcroft Institute and STFC/DL/ASTeC, Daresbury, UK
L. Cosentino, P. Finocchiaro, A. Pappalardo, INFN-LNS, Catania, Italy

THIN FOIL-BASED SECONDARY EMISSION MONITOR FOR LOW INTENSITY, LOW ENERGY BEAM PROFILE MEASUREMENTS*

J. Harasimowicz†, C.P. Welsch, Cockcroft Institute and University of Liverpool, UK
J.L. Fernandez-Hernando, Cockcroft Institute and STFC/DL/ASTeC, Daresbury, UK
L. Cosentino, P. Finocchiaro, A. Pappalardo, INFN-LNS, Catania, Italy

Abstract

A foil-based secondary emission monitor (SEM) was developed for beam profile measurements at the Ultra-low energy Storage Ring (USR) that will be installed at the future Facility for Low-energy Antiproton and Ion Research (FLAIR) in Darmstadt, Germany. Simulations of the optimised design of the monitor are presented. Furthermore, its usability for the low energy antiproton ($\bar{p}$) beam profile monitoring is discussed.

INTRODUCTION

A thin foil-based secondary emission monitor (SEM) was developed to measure profiles of low energy, low intensity beams at the Ultra-low energy Storage Ring (USR) [1]. The detector consists of a grounded mesh and an aluminium foil on negative potential, a chevron type microchannel plate (MCP) with a phosphor screen and a CCD camera registering the image, see Fig. 1.

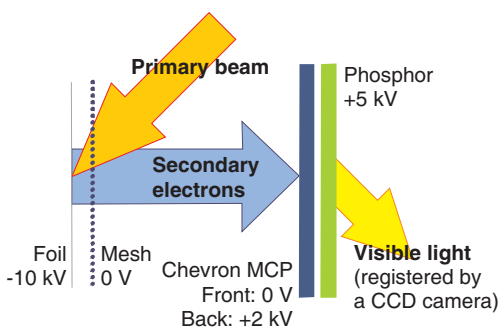

Figure 1: Schematic diagram of SEM with maximum applicable voltages.

The primary beam passes through the mesh at 45° and ejects eV-range secondary electrons (SE) from the foil surface. These secondaries are accelerated towards the mesh placed 5 mm away by the negative voltage applied to the foil. By the time they reach the mesh, they are already highly directional and fly towards the detector located ca. 50 mm away. There they are multiplied by the MCP and converted to visible light by the phosphor producing an image which can be registered by a CCD camera.

* Work supported by the EU under contract PITN-GA-2008-215080, by the Helmholtz Association of National Research Centers (HGF) under contract number VH-NG-328, and GSI Helmholtz Centre for Heavy Ion Research.

† Janusz.Harasimowicz@liverpool.ac.uk

ELECTROSTATIC SIMULATIONS

The influence of the applied voltages on low energy beams and on secondary electrons was studied with the use of SIMION [2].

Primary keV Beams

A simple model with only a foil, a parallel mesh placed 5 mm away made of 25 µm wires with 80 wires per inch and an MPC/phosphor assembly located 47 mm further away was simulated. It was tested with the maximum voltages of -10 kV for the foil, +2 kV for the MCP and +5 kV for the phosphor. Fig. 2 shows the effect of the unshielded SEM on 300 keV and 20 keV beams delivered by the USR. The influence on 300 keV particles was noticeable, yet small, with the beam shift reaching less than 0.7 mm. However, 20 keV protons were displaced by ca. 8 mm while 20 keV antiprotons or H^- ions did not reach the foil at all.

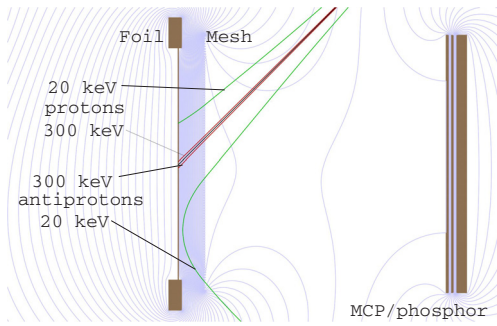

Figure 2: Influence of the unshielded SEM on the low energy beams of the USR.

The setup was improved by adding a shield as shown in Fig. 3. This time, the USR beams could reach the detector and were affected mainly in the region between the foil and the mesh. A displacement of less than 0.1 mm for 300 keV particles, less than 1 mm for 20 keV protons and about 3-5 mm, depending on the position with respect to the wires of the mesh, for single-charged negative particles was observed. The results were produced for monoenergetic pencil beams emitted at 45° to the foil and -10 kV accelerating voltage. At this voltage, a small variation in the initial conditions was significant for 20 keV antiprotons or H^- ions and differences as small as 2% in angle (1°) or energy (400 eV) were critical for the beam observation. In comparison, about 10% and 20% variation in energy was acceptable at

-9 kV and -8 kV, respectively. Also the beam displacement was reduced 1.5-2 times as compared to the -10 kV case.

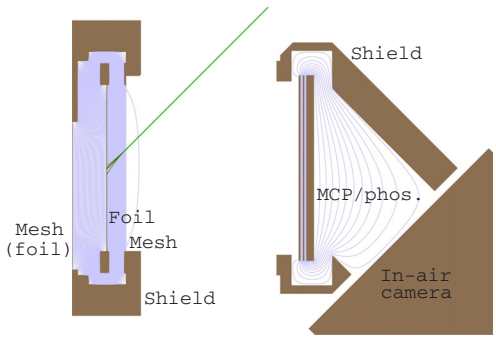

Figure 3: Influence of the shielded SEM on the low energy beams of the USR.

Secondary Electrons

The angular distribution of the emitted electrons tends to obey a cosine-law independently of the incidence angle of the primary beam [3]. Also the peak energy at about 2.1 eV seems not to depend on the combination of the projectile and target used [3, 4]. However, other important parameters, including the electron yield and the energy spectrum shape, are strongly influenced by many factors. These include the energy and angle of incidence of the projectile or electric field near the surface, but also the purity, oxidization and surface roughness of the target. Therefore, it is not easy to properly characterise the emission of SE and the following considerations are only approximate.

A Monte Carlo routine was written for SIMION to generate secondary electrons with the energy spectrum for a clean aluminium surface bombarded with 500 keV protons [4], which should be very similar also for lower energies, and a cosine-like angular distribution. A point source of SE was defined at the foil surface and the resulting spatial distribution was recorded at the MCP plane. Initially, the mesh was approximated by a plane of zero voltage fully transparent to particles ("ideal mesh"). For such a configuration, the standard deviation σ of the simulated distribution was about 0.9 mm for -10 kV applied to the foil. With the total yield of roughly 1 electron per proton [4], it means about $8 \cdot 10^{-2}$ e$^-$/mm^2/proton at the MCP surface.

A more realistic model with a 80 wires per inch (wpi) mesh was also studied. In this case, the point source model was not useful, because the simulated distributions were strongly affected by the position of the wires with respect to the source. To avoid artificial structures in the image and to simulate a more realistic case, a Gaussian source with σ = 1 mm was defined. SE reaching the MCP were recorded and a standard deviation was derived for a range of accelerating voltages, see Fig. 4. Broadening of the beams with the decreasing voltage can be observed, but variations in σ for higher voltages were not significant.

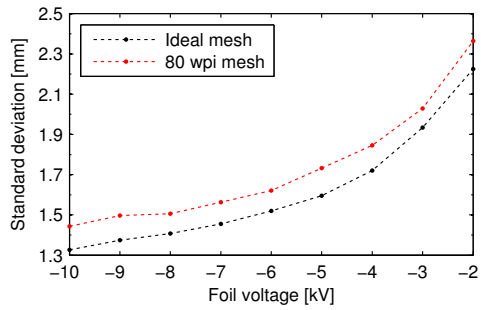

Figure 4: Simulated profiles of SE emitted from a Gaussian source with σ = 1 mm and recorded at the MCP surface for different accelerating voltages.

CONSIDERATIONS FOR ANTIPROTONS

It is not easy to model the behaviour of the SEM bombarded with low energy antiprotons because of the variety of events which occur due to and after the annihilation [5, 6]. A combined charge signal from all of the effects would be extremely complicated and rather impossible to simulate in any precise way. Existing Monte Carlo codes could provide only a simplified picture of the processes inside the SEM without taking into account many substantial aspects, like the creation of eV-scale secondaries. Most importantly, computer codes are limited by the experimental data which are not yet complete for low energy antiprotons. However, it is clear that the annihilation of antiprotons will increase the number of particles reaching the MCP and therefore will affect the observed image. A more quantitative assumption could be based on a simplified Monte Carlo model, but with the above limitations kept in mind.

Fluka [7] was used to estimate the number of particles generated in a collision of 300 keV antiprotons with a 100 µm aluminium foil. A 20 mm diameter beam with a uniform distribution contained $2 \cdot 10^7$ antiprotons and was fully stopped in the foil placed at 45°. No additional materials or electric fields were introduced. The resulting fluence of particles created in the process is shown in Fig. 5.

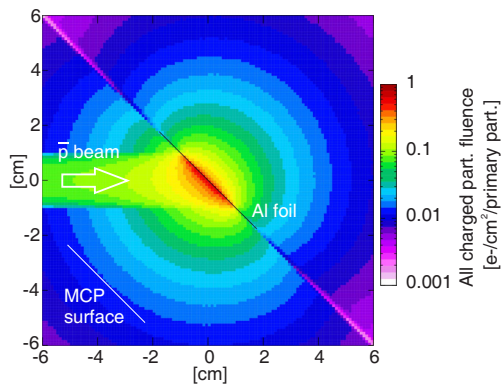

Figure 5: Fluka simulated fluence of charged particles created in the annihilation of 300 keV antiprotons.

From the simulations, it looks like approximately $6{\cdot}10^{-5}$ charges/mm^2/$\bar{p}$ will reach the MCP surface. What is not considered, however, are e.g. the eV-scale particles critical for the SEM operation. The annihilation products and their energy spectra simulated with Fluka are shown in Fig. 6.

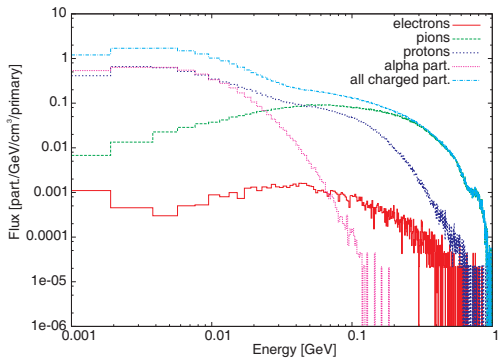

Figure 6: Energy spectra of charged particles following the annihilation of 300 keV antiprotons in aluminium as simulated with Fluka.

An influence of the annihilation could be minimised by the use of an ultra-thin foil with thickness smaller than the range of the projectiles in matter, i.e. <3 µm for 300 keV and <0.2-0.3 µm for 20 keV [8]. Such foils, however, are expensive and very difficult to produce and handle. Most of them would be too fragile to be used unsupported for a diameter of about 50 mm required by the SEM geometry. A low density support mesh could be used, but the annihilation products would be present anyhow due to the interaction of the $\bar{p}$ beam with the SEM components, and the halo particles with the vacuum vessel and the SEM shield. The resulting image in such a configuration is not easy to predict and an experimental verification is required.

Another idea is to use the MCP directly in the beam path. Up to 10^5 antiprotons over 10 ms every >1 minute were successfully imaged with the MCP at CERN AD [9]. However, larger amounts have been observed to saturate the detector due to high energy secondary particles produced in the annihilation at the detector surface. They excite additional cascades, enhancing the MCP gain and therefore limit its application to low intensity $\bar{p}$ beams.

DESIGN AND MEASUREMENTS

The final design of the detector is shown in Fig. 7. The foil/mesh assembly as well as the MCP/phosphor are shielded as discussed previously. The distance between the MCP surface and the foil was set to 52 mm in order to maximise the beam diameter accepted by the detector. In addition, the design was made flexible to enable the use of two configurations, the SEM and a stand-alone MCP.

It has been arranged to first test the detector with low energy beams at INFN-LNS in Italy where protons and ions can be delivered at a variety of energies and intensities. Secondly, preparations have been done to integrate the

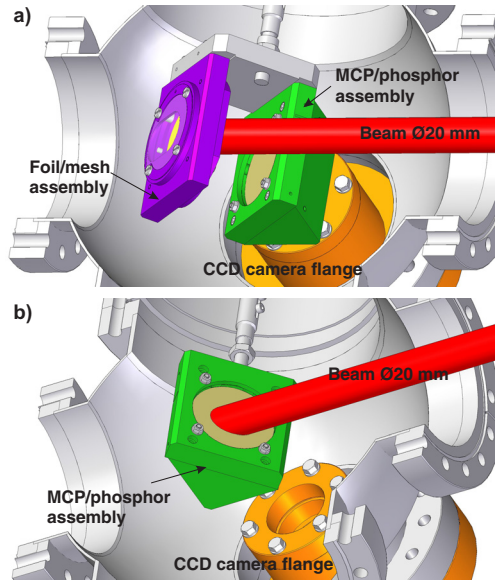

Figure 7: Two configurations of the detector: a) foil-based SEM, b) MCP directly in the beam path.

SEM in the beamline of the Antimatter Experiment: Gravity, Interferometry, Spectroscopy (AEgIS) at CERN. This has required a careful preparation of the overall setup to get conditions that are close enough to those expected at the USR.

REFERENCES

[1] C. P. Welsch et al., "An Ultra-low-energy Storage Ring at FLAIR", Nucl. Instrum. Meth. A 546(3), p. 405-417 (2005).

[2] SIMION 8.0, http://www.simion.com.

[3] P. N. Ostroumov et al., "Design and test of a beam profile monitoring device for low intensity radioactive beams", Rev. Sci. Instrum. 73, p. 56-62 (2002).

[4] D. Hasselkamp et al., "Particle Induced Electron Emission 2", Springer-Verlag (1992).

[5] M. Inokuti, "Interactions of antiprotons with atoms and molecules", Int. J. Rad. Appl. Instrum. D 16, p. 115-123 (1989).

[6] H. Imao et al., "Observation of Ultra-Slow Antiprotons using Micro-channel Plate", AIP Conf. Proc. 1037, p. 311-317 (2008).

[7] Fluka, http://www.fluka.org.

[8] S. P. Møller et al., "Measurement of the Barkas effect around the stopping-power maximum for light and heavy targets", Nucl. Instrum. Methods Phys. Res. B 122, p. 162-166 (1997).

[9] G. B. Andresen et al., "Antiproton, positron, and electron imaging with a microchannel plate/phosphor detector", Rev. Sci. Instrum. 80, 123701 (2009).